2004

Effects of sham air and cigarette smoke on A549 lung cells: Implications for iron-mediated oxidative damage

Jonathan J. Mayo

Pete Kohlhepp

Dianzheng Zhang
Philadelphia College of Osteopathic Medicine, DianzhengZh@pcom.edu

Joy J. Winzerling

Am J Physiol Lung Cell Mol Physiol 286: L866–L876, 2004;
10.1152/ajplung.00268.2003.

Effects of sham air and cigarette smoke on A549 lung cells: implications for iron-mediated oxidative damage

Jonathan J. Mayo, Pete Kohlhepp, Dianzheng Zhang, and Joy J. Winzerling
Department of Nutritional Sciences, The University of Arizona, Tucson, Arizona 85721

Submitted 31 July 2003; accepted in final form 3 December 2003

Mayo, Jonathan J., Pete Kohlhepp, Dianzheng Zhang, and Joy J. Winzerling. Effects of sham air and cigarette smoke on A549 lung cells: implications for iron-mediated oxidative damage. *Am J Physiol Lung Cell Mol Physiol* 286: L866–L876, 2004; 10.1152/ajplung.00268.2003.—Inhalation of airborne pollution particles that contain iron can result in a variety of detrimental changes to lung cells and tissues. The lung iron burden can be substantially increased by exposure to cigarette smoke, and cigarette smoke contains iron particulates, as well as several environmental toxins, that could influence intracellular iron status. We are interested in the effects of environmental contaminants on intracellular iron metabolism. We initiated our studies using lung A549 type II epithelial cells as a model, and we evaluated the effects of iron dose and smoke treatment on several parameters of intracellular iron metabolism. We show that iron at a physiological dose stimulates ferritin synthesis without altering the transferrin receptor (TfR) mRNA levels of these cells. This is mediated primarily by a reduction of iron regulatory protein 2. Higher doses of iron reduce iron regulatory protein-1 binding activity and are accompanied by a reduction in TfR mRNA. Thus, for A549 cells, different mechanisms influencing IRP-IRE interaction allow ferritin translation in the presence of TfR mRNA to provide for iron needs and yet prevent excessive iron uptake. More importantly, we report that smoke treatment diminishes ferritin levels and increases TfR mRNA of A549 cells. Ferritin serves as a cytoprotective agent against oxidative stress. These data suggest that exposure of lung cells to low levels of smoke as are present in environmental pollutants could result in reduced cytoprotection by ferritin at a time when iron uptake is sustained, thus enhancing the possibility of lung damage by iron-mediated oxidative stress.

iron; lung cells; iron regulatory protein 2; ferritin; transferrin receptor

LUNG TISSUES ARE VULNERABLE to environmental pollutants, and inhalation of airborne pollution particles results in a variety of detrimental changes (26, 41). Available evidence indicates that iron-mediated oxidative stress is, in part, responsible for these changes (22, 26, 32). A role for iron has been implicated in numerous lung diseases (33, 42), and body iron status can influence pulmonary disease (16, 43).

Iron delivery to most mammalian cells occurs by specific, high-affinity transferrin receptors (TfRs) that bind blood diferric transferrin (40). Intracellular iron is found stored as ferritin in a labile iron pool or incorporated in a variety of proteins. Intracellular iron homeostasis is maintained primarily by the expression of TfRs (iron acquisition) and ferritin (iron storage; see Ref. 10). Synthesis of these proteins is controlled at the translational level by the binding of the iron regulatory proteins (IRP), IRP1 and IRP2, to iron responsive elements (IREs), mRNA stem loop regulatory control sites. IRP interaction with an IRE in the 5′-untranslated region (UTR) of ferritin subunit mRNA prevents full assembly of the ribosomal apparatus and blocks ferritin synthesis (36). IRP interaction with multiple IREs in the 3′-UTR of the TfR mRNA protects the mRNA from degradation and allows continued translation of the message. Thus, when iron is low, TfRs are synthesized to increase iron uptake. However, when iron is abundant, an iron sulfur cluster (4Fe-4S) forms in the core of IRP1 and prevents IRE binding (5, 21), whereas IRP2 is rapidly degraded (5, 21). This results in decreased IRP-IRE interaction, ferritin synthesis, and TfR mRNA degradation. Other factors that influence this pathway include nitric oxide, hydrogen peroxide, hypoxia/reoxygenation, and hyperoxia (reviewed in Refs. 1, 9, 10, 30).

Lung cells can acquire iron from TfRs (15). In addition, iron uptake from airborne particles can occur by phagocytosis or by the divalent cation transporter, DCT-1 (17). The lung iron burden is substantially increased by exposure to cigarette smoke (37). An estimated 1.2 μg of iron can be delivered from a pack of unfiltered cigarettes, a portion of which remains in the respiratory cells (49). Iron, delivered from smoke, can induce oxidative stress in lung tissues in vivo with adverse consequences (31). Lung cells also are unique in that they are routinely exposed to changes in the levels of oxygen and oxygen tension.

We are interested in the effects of environmental contaminants on intracellular iron metabolism. Pollution particles that contain iron can induce ferritin synthesis in lung A549 type II epithelial cells (14, 38). As a first step, we have used A549 cells as a model to determine the effects of iron dose and smoke treatment on parameters of intracellular iron metabolism. We show that iron within the physiological dose range stimulates ferritin synthesis without altering the TfR mRNA levels of these cells. This appears mediated by a reduction of IRP2. We also report that limited smoke exposure lowers ferritin levels and increases TfR mRNA levels of A549 cells. Low ferritin levels in the presence of continued iron uptake with prolonged exposure to smoke could render lung cells vulnerable to oxidative stress.

MATERIALS AND METHODS

Cell cultures and experimental protocols. A549 type II lung epithelial cells were obtained from the American Type Culture Collection (Manassas, VA). Stock cell cultures were maintained in RPMI medium 1640 (Invitrogen, Carlsbad, CA) supplemented with 5% heat-inactivated FBS (Gemini Bio-Products, Calabasas, CA) and 100 U/ml penicillin G, 100 μg/ml streptomycin sulfate, and 0.25 μg/ml amphotericin B. Cells for stock cultures and all experiments were incubated at 37°C in a water-jacketed incubator (10% humidity, 95% air-5% CO_2 atmosphere). All experiments were performed with cells

Address for reprint requests and other correspondence: J. Winzerling, Dept. of Nutritional Sciences, P.O. Box 210038, The Univ. of Arizona, Tucson, AZ 85721.

The costs of publication of this article were defrayed in part by the payment of page charges. The article must therefore be hereby marked "*advertisement*" in accordance with 18 U.S.C. Section 1734 solely to indicate this fact.

at >80% confluence in 75-cm^2 tissue culture flasks (Corning, Corning, NY). At the start of each experiment, the complete medium was removed. The cells were washed two times with Hanks' balanced salt solution (HBSS) and incubated for 1 h in serum-free medium. After incubation, the medium was replaced with fresh serum-free medium, and the appropriate treatment was administered.

Dose-response experiments. Ferric ammonium citrate (FAC, 18.3% iron, 327.4 g/mol; Sigma, St. Louis, MO) and desferoxamine mesylate (DES; Sigma) were diluted in HBSS. Ferric was chosen for these studies because ferrous is readily oxidized in the presence of oxygen in an aqueous environment. HBSS was added to control cells so that all flasks had the same concentration of HBSS, RPMI 1640 medium, and the same final volume. For dose-response experiments, cells were incubated in 0, 25, 50, 75, and 100 μM FAC or 100 μM FAC and 100 μM DES for 18 h. After treatment, the medium was removed and overlayered with 0.2% butylated hydroxytoluene (BHT), flash-frozen in liquid nitrogen, and stored at −80°C for thiobarbituric acid reactive species assay (TBARS). Cell monolayers were washed two times with HBSS and incubated at 37°C with 0.25% trypsin/1.0 mM EDTA (Invitrogen) for 5 min. Cells were rinsed gently from the flask in HBSS (5 ml) and centrifuged in conical tubes (1,800 *g*, 5 min). Cell pellets were washed and suspended in HBSS (5 ml). Cell viability was determined in triplicate by CellTiter 96 Aqueous One Solution Cell Proliferation Assay (Promega, Madison, WI). Total cell number was determined in triplicate using the LIVE/DEAD Viability/Cytotoxicity Kit (Molecular Probes, Eugene, OR). One milliliter (~1.5×10^6 cells) of the cell suspension was taken from each sample for RNA isolation. The remaining cells were centrifuged, and the cell pellet was stored at −80°C for cytoplasmic extraction.

Smoke experiments. A filterless IR4F research grade cigarette (University of Kentucky, Tobacco and Health Research Institute, Lexington, KY) was placed through a gasket in the top of a 50-ml Corning polyethylene tube with a luer-lok fitting at the bottom. Attached to the luer-lok was a tube with an inline Hepa-Vent 0.3-μm glass microfiber filter (Whatman International, Maidstone, UK) followed by a Bel-Art Products (Pequannock, NJ) flowmeter attached to regulated, compressed, breathing-quality air (22% oxygen; US Airweld, Phoenix, AZ). Smoke or air (sham) was injected in the flask at a flow rate of 6 ml/s for delivery of 30 ml. The flasks were closed and the cells incubated for the designated time interval. At the appropriate time, the cells were harvested as described above; viability was determined by the trypan blue dye exclusion assay.

Cytoplasmic extracts. Cell pellets were thawed for 10 min on ice and suspended in an equivalent packed cell volume of hypotonic buffer (10 mM HEPES, pH 7.9, 1.5 mM $MgCl_2$, 10 mM KCl, freshly added 0.2 mM PMSF, and 0.5 mM DTT; see Ref. 4). Cells were gently homogenized for 20 s. Nuclei were removed at 3,300 *g* for 15 min and 4°C. Cellular membranes were removed by centrifugation of the supernatants at 100,000 *g* for 1 h at 4°C. Cytoplasmic extracts were flash-frozen in small aliquots and held at −80°C until use. Protein was determined by Bradford (6) assay.

Electrophoretic mobility shift assay. Transcripts of the human ferritin heavy-chain IRE were obtained using the template provided by the RNA Gel Shift Kit (MBI Fermantas, Amherst, NY) and were labeled with [α-^{32}P]CTP (50 μCi, >3×10^6 mCi/mmol; Amersham). After transcription, transcripts were precipitated in ethanol, suspended in diethyl pyrocarbonate-treated water, and quantified for [^{32}P]CTP incorporation. EMSA was conducted as described by others (44). Briefly, cytoplasmic extract (5 μg) and labeled transcript of human ferritin heavy-chain IRE (50 fmol) were incubated in 25 mM HEPES, 150 mM CH_3COOK, 1.5 mM $MgCl_2$, 10 mM cysteine, and 5% glycerol for 30 min [room temperature (RT)]. RNase T_1 (1 U/ml) was then added to degrade excess probe, and the mixture was incubated for 10 min (RT). Heparin (3 mg/ml; Sigma) was added, and the reaction was incubated for 10 min (RT). The samples were separated on a 6.5% polyacrylamide gel. The gel was dried, and binding activity was assessed by autoradiography (Custom X-ray Imaging Service, Phoenix, AZ), measured by laser scanning, and quantified using ImageQuaNT (Molecular Dynamics). IRP1 was distinguished from IRP2 by supershift assay by adding 15 μg of anti-rat IRP1-specific antiserum (a kind gift from Dr. Richard Eisenstein, Madison, WI; see Ref. 12) after the initial reaction (10 min, 4°C). Measurement of spontaneous binding activity was determined in the absence of cysteine.

Immunoblot analysis. IRP2 was determined from cytoplasmic extract proteins separated by SDS-PAGE on a 7% homogeneous SDS Mini gel at 100 volts for 1 h at RT. Ferritin subunits were resolved by SDS-PAGE on an 18.5% homogeneous SDS Mini gel at 60 volts overnight at 4°C. Proteins were transferred to a nitrocellulose membrane using a Mini Trans-Blot Transfer apparatus according to the manufacturer's specifications. Ponceau S confirmed efficient transfer of the proteins. The nitrocellulose membrane was blocked for 1 h in modified Blotto (7% nonfat milk-3% BSA-0.05% Triton X-100-PBS, pH 7.4) at RT. Next, the membrane was incubated with either anti-rat IRP2-specific rabbit antiserum (1:2,000 vol/vol; see Ref. 24) or anti-human ferritin sheep antiserum (1:250 vol/vol; Binding Site, San Diego, CA) in dilution buffer (3% BSA-0.05% Triton X-100-PBS, pH 7.4) for 2 h at RT. The membrane was washed three times in buffer (0.05% Triton X-100/PBS, pH 7.4). IRP2 was measured by incubating the membrane with anti-rabbit alkaline phosphatase conjugate antibody (Jackson Immuno, West Grove, PA) and was developed in substrate according to the manufacturer's methods (Bio-Rad, Hercules, CA). Ferritin was measured by enhanced chemiluminescence using an anti-sheep horseradish peroxidase-conjugated antibody and the SuperSignal West Pico chemiluminescent Kit (Pierce, Rockford, Il) and exposure to Blue XB-1 film (Eastman Kodak, Rochester, NY). IRP2 and ferritin subunit volumes were measured by laser scanning and quantified using ImageQuaNT software (Molecular Dynamics).

Thiobarbituric acid assay. The extent of lipid peroxidation was determined by thiobarbituric acid (TBA) reaction according to Winzerling et al. (51). Before thawing, the culture medium was overlayered with 0.2% BHT (100 μl). Freshly diluted malondialdehyde was used as a standard.

Semiquantitative RT-PCR. Total RNA was isolated from 1.5×10^6 cells using the RNeasy Mini Kit (Qiagen, Valencia, CA). Samples were treated with Amplification Grade DNase I (1 U/10 μl RNA) for 15 min (RT) and then heated (65°C, 10 min) to inactivate the enzyme. All RNA samples were transcribed using Superscript2 Reverse Transcriptase (Invitrogen) according to the manufacturer's instructions. The specific primers for the PCR reactions were as follows: IRP1: 5′-TGGGGTGTCGGTGGTATTG-3′ and 3′-GGCAGCAATGACCACAGAAC-5′; TfR: 5′-ACAGCACAG ACTTCACCAGC-3′ and 3′-CCAGATGAGCATGTCCAAAG-5′; IRP2: 5′-TGTGCAATACAGAATGCACC-3′ and 3′-GGAAGAGGAGGTCTTTTTCT-5′; ferritin heavy chain: 5′-AAGCTGCAGAACCAACGAGG-3′ and 3′-TGGTGACC AGGGAAGTCAC-5′; and ferritin light chain: 5′-GACCGCGATGATGTGGCT-3′ and 3′-GCCATGGCAGCTTTCATG-5′. PCR reactions were conducted using *Taq* DNA Polymerase (Invitrogen) with the buffers provided for 30 cycles of 30 s at 94°C, 1 min at the appropriate annealing temperature, followed by 1 min at 72°C. QuantumRNA 18S Internal Standard kit (Ambion, Austin, TX) was used as an internal control. All primer pairs were optimized with the 18S Primer/Competimer mix for similar band intensity. PCR products were separated on 1.5% agarose gels and visualized using ethidium bromide stain. Digital images were assessed using a charge-coupled device camera (Ultra Lum, Carson, CA) and quantified with ImageQuaNT software. Data were analyzed as a ratio of the desired product to the 18S internal standard. All PCR products were cloned and sequenced to determine that the product sequence was that of the desired message.

Statistics. Treatment differences were determined by one-way ANOVA using the Dunn-Bonferroni posttest for comparison of selected data sets or where appropriate by unpaired *t*-test. A minimum of two sets of three experiments each was done to assure reproducibility. Graphed data represent the means ± SE of three experiments.

RESULTS

Physiological iron dose induces ferritin synthesis without decreasing TfR mRNA. Iron delivered as 25 μM FAC induced maximal ferritin synthesis of A549 cells, and cells exposed to higher doses showed no further increase (Fig. 1*A*). The effects of iron were abrogated by the addition of DES, indicating that iron was responsible for the increase in ferritin synthesis seen at 100 μM FAC. A549 cells synthesized more ferritin light chain than heavy chain in response to iron treatment. Our findings are in agreement with others who have demonstrated that ferric chelated to low molecular compounds enters lung cells (14) and that iron at low doses stimulates ferritin synthesis, but the response is not linear with increasing dose (44). The iron concentration in 25 μM FAC approximates that of normal human serum iron (49). It should be noted that, although iron concentrations are in this range, iron here is coordinated with citrate and not with transferrin to more closely resemble a form of iron that could be available from airborne particulate matter (32).

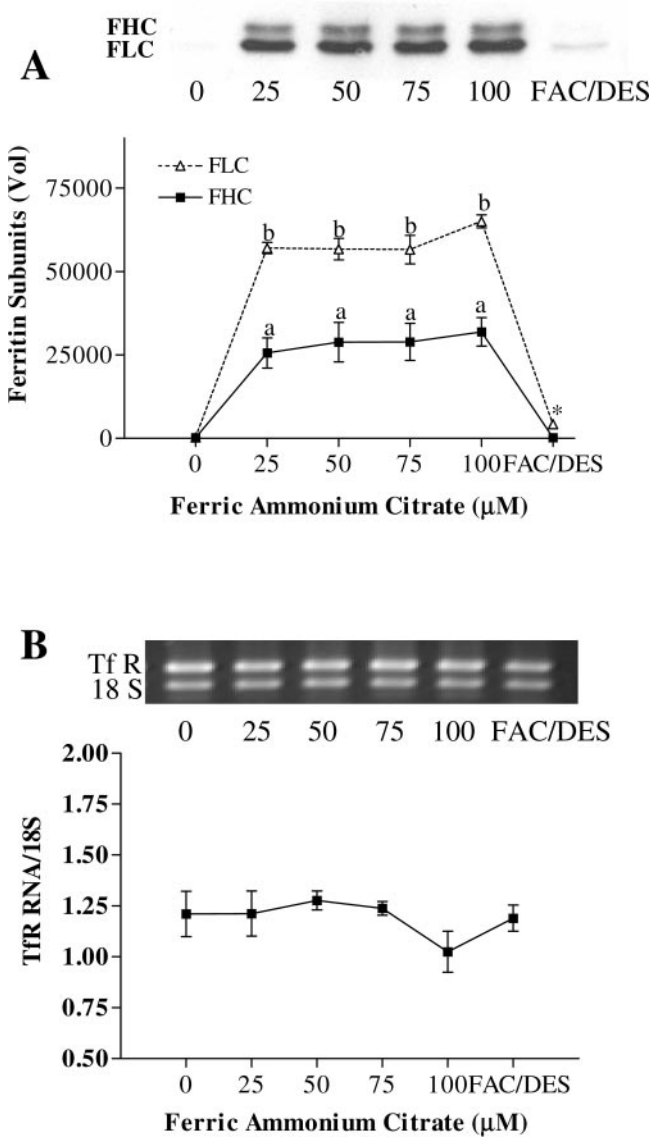

Fig. 1. Ferritin synthesis and transferrin receptor (TfR) mRNA respond differently to iron dose. A549 cells were incubated in culture medium with 0–100 μM ferric ammonium citrate (FAC) or 100 μM FAC with 100 μM desferoxamine (DES) for 18 h. *A*: physiological iron dose induces maximal ferritin synthesis in A549 lung cells. Cells were harvested, and immunoblots were conducted and analyzed as described in MATERIALS AND METHODS. FHC, ferritin heavy chain; FLC, ferritin light chain. [a]Significantly different from 0 μM FAC, $P < 0.01$. [b]Significantly different from 0 μM FAC, $P < 0.001$. [*]Significantly different from 100 μM FAC, $P < 0.001$. *B*: TfR mRNA levels are reduced at high iron levels. Cells were harvested, and semiquantitative RT-PCR was done as described in MATERIALS AND METHODS. Data were analyzed as a ratio of TfR product to the 18S internal standard. Blots on *top* represent one experiment; graphed data represent means ± SE for 3 experiments.

Others have shown that A549 cells synthesize TfRs (15), and studies in other cell types indicate that TfR mRNA levels correlate positively with protein expression and are sensitive to iron administration (40). Treatment of cells with 25–75 μM FAC did not significantly reduce TfR mRNA levels (Fig. 1*B*). Receptor mRNA levels declined at 100 μM FAC treatment. These results were reproducible in a second set of studies. We conclude that low and moderate doses of iron increase ferritin synthesis but do not result in TfR mRNA degradation. Thus it is possible for these cells to maintain iron stores without downregulating the TfR mRNA at these iron levels. For these experiments, cell numbers did not differ significantly among flasks, as assessed by the ethidium assay. Iron treatment reduced cell viability to ~70% of controls, as measured by Formazan absorbance, but the effect was not iron-dose responsive (data not shown).

Low iron dose reduces IRP2 binding activity. In cellular studies reported to date, iron administration decreases IRP interaction with the IRE, and this allows translation of ferritin but renders the TfR mRNA vulnerable to degradation (2, 10). Binding activity is customarily measured with (total) and without (spontaneous) reducing agent. Total binding activity reflects the relative contributions of both IRP2 and IRP1, as well as the levels of IRP1 available in an oxidized form that does not bind to the IRE (10, 24). Although we found that both total and spontaneous IRP/IRE binding activity declined with iron treatment relative to untreated cells (Fig. 2*A*), this decrease reached significance only at 100 μM FAC for spontaneous binding activity ($P < 0.05$). From these data, we conclude that A549 cells have a high level of binding activity when the cells are incubated 18 h in the absence of serum or treated with DES in the presence of FAC. The addition of iron at physiological dose or slightly greater levels is not sufficient to significantly reduce binding activity; higher levels are required. This could explain why the TfR mRNA is preserved after iron administration within this range. However, we wondered what could account for the increased ferritin synthesis we observed.

Studies by others have shown that binding affinity of the ferritin IRE is greater for IRP2 than for IRP1 (28). Lung cells express messages for both IRP1 and IRP2, but levels are considerably lower than those of other tissues (20). We determined the relative contribution of each IRP to binding activity using EMSA supershift assays (Fig. 2*B*). IRP1 binding activity was greater than that contributed by IRP2. IRP1 binding activity declined at 100 μM FAC (Fig. 2*B*, *top*). In contrast IRP2 levels were low, but detectable, in untreated cells (Fig. 2*B*, *bottom*). However, treatment of cells with 25 μM FAC resulted in nearly a complete loss of measurable IRP2 binding activity. We also found that mRNA levels for the ferritin subunits did not differ significantly with iron dose (data not

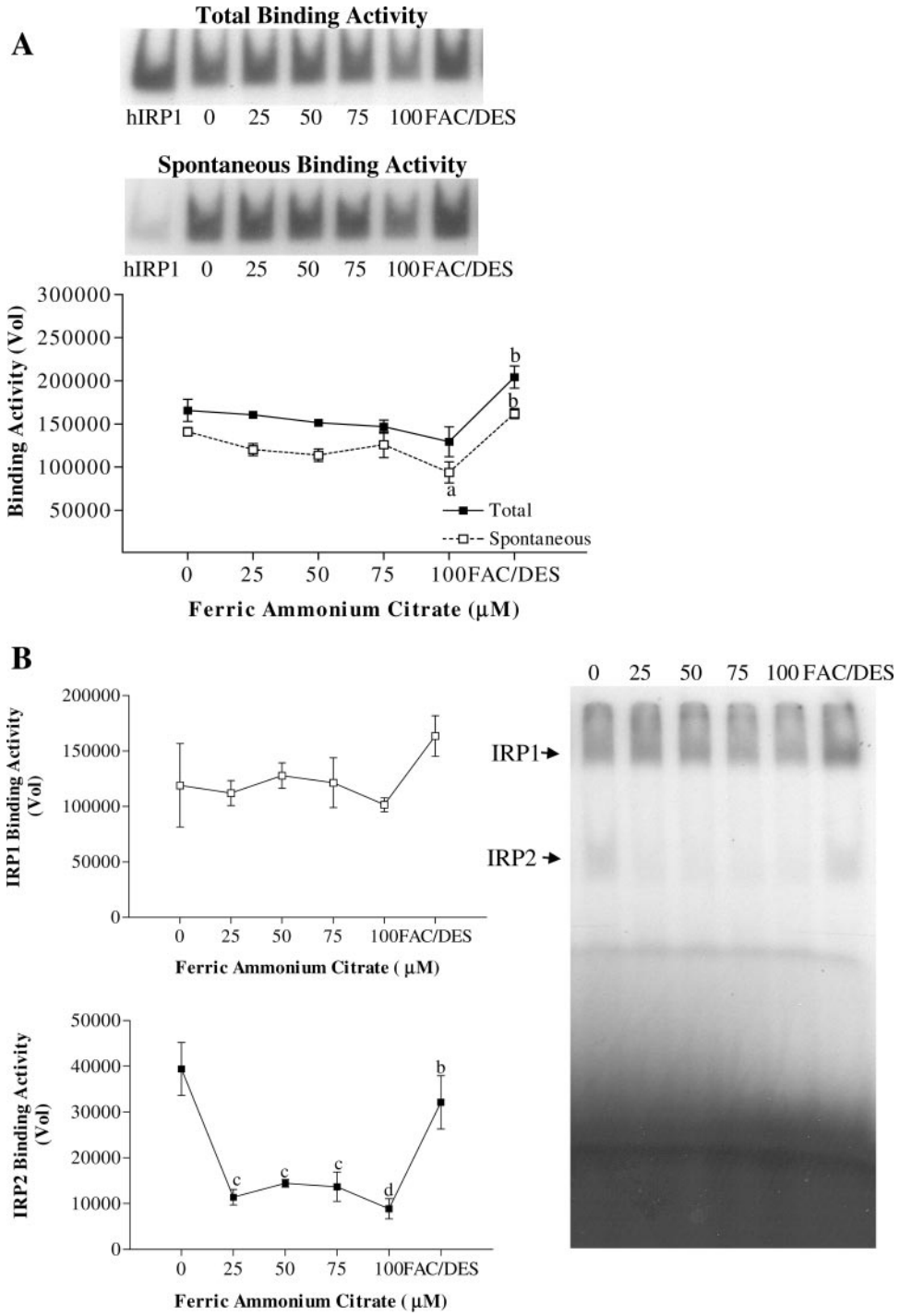

Fig. 2. Electrophoretic mobility shift assay (EMSA) of iron responsive element (IRP)-iron regulatory element (IRE) binding activity of A549 cells treated with iron. A549 cells were incubated in culture medium with 0–100 μM FAC or 100 μM FAC with 100 μM desferoxamine for 18 h. Cells were harvested, and EMSAs were conducted and analyzed as described in MATERIALS AND METHODS. *A*: total and spontaneous binding activity declines with iron treatment. *Top*, representative EMSA for either total or spontaneous binding. [b]Significantly different from 100 μM FAC, $P < 0.01$. *B*: iron administration differentially regulates IRP1 and IRP2 binding activity. A representative EMSA using IRP1 antiserum is shown on *right*. [b]Significantly different from 100 μM FAC, $P < 0.05$. [c]Significantly different from 0 μM FAC, $P < 0.01$. [d]Significantly different from 0 μM FAC, $P < 0.001$.

shown). These data taken together show that iron at a physiological dose significantly reduces IRP2 binding activity of A549 cells, whereas IRP1 binding activity is modified only with exposure to higher iron levels and is sustained even at 100 μM FAC. These findings indicate that ferritin levels of A549 cells are sensitive to IRP2 binding activity and that a small change in this parameter can significantly upregulate ferritin synthesis, whereas TfR mRNA levels more closely reflect changes in IRP1 binding activity for these cells.

We were surprised that IRP1 binding activity levels were not decreased at the low iron concentrations. Oxidative stress has been shown to regulate IRP1 binding activity (reviewed in Refs. 9, 10, 24). In addition, recently reported data showed that iron administered in the 1.5- to 20-μM range (ferric chloride) resulted in a decline in IRP1 binding activity, but higher concentrations increased IRP1 binding activity (39). This phenomenon was cell-type specific and was attributed to upregulation of IRP1 by iron-mediated oxidative stress. We found no lipid peroxide byproducts for any iron dose (data not shown).

Smoke exposure significantly reduces viable cells. We exposed A549 cells to 30 ml of smoke for time intervals to 22 h. Cell counts were used to determine the number of cells per

flask and are expressed as a percentage of the number of untreated cells at 0 h (controls, Fig. 3*A*). Smoke significantly reduced cell numbers at all time intervals. Because the initial numbers of cells per flask did not decline as determined by ethidium assay (Fig. 3*B*), the low numbers of cells in smoke-treated samples resulted from cell lysis. Viability was determined by trypan blue exclusion, not Formazan, because we thought that redox active compounds present in smoke might influence mitochondrial activity. The percentage of viable sham cells did not differ significantly with time relative to controls (Fig. 3*C*). Viability of the cells remaining in the smoke treatment groups also was not compromised at the lower time intervals but was significantly reduced at 22 h relative to controls or to sham cells.

Smoke reduces ferritin levels and prevents a decline in TfR mRNA. Surprisingly, sham treatment of cells resulted in a dramatic and significant increase in ferritin levels at 4 and 6 h (Fig. 4*A*). Because the medium used during these experiments was serum free, we expected little upregulation of ferritin in sham cells. By 22 h, ferritin of sham cells declined significantly relative to values at 4 and 6 h but remained significantly greater than controls. Importantly, the increase in ferritin synthesis observed for sham cells was significantly diminished by smoke (Fig. 4*A*).

Sham air also reduced TfR mRNA levels significantly by 4 h (Fig. 4*B*). In contrast, TfR mRNA levels did not change for cells treated with smoke. From these experiments, we conclude that sham air flow increases ferritin synthesis and decreases TfR mRNA in A549 cells, and this response is diminished by smoke. Similar results were found for studies conducted without an inline filter.

Sham air introduced over lung cells significantly reduces IRP2 levels. We expected that total binding activity would decline at the early time intervals to account for the changes in ferritin synthesis we observed. Total binding activity was very low in sham samples at 4 and 6 h but increased significantly at 22 h (Fig. 5, *A* and *B*). Smoke prevented the slight increase in total binding activity at 6 h and significantly diminished the increase at 22 h relative to controls or sham cells at this time interval. Spontaneous binding activity also followed these trends (Fig. 5*C*). In preliminary work, we found that cells preincubated in serum-free medium could not tolerate smoke treatment. We think the low levels of total binding activity we observed at the early time intervals reflected overnight incubation in serum-containing medium before initiating treatment. The dramatic increase in total binding activity observed at 22 h corresponds with the observed decline in ferritin synthesis at this time interval and could well reflect incubation of the cells in serum-free medium.

Because increased ferritin mRNA levels also could account for the increase in ferritin we observed after sham air treatment, we evaluated messages for both subunits. Neither mRNA was increased by sham air nor did mRNA levels vary as a result of smoke treatment (data not shown). Although we conducted supershift assays, we found that the levels of binding activity at the early time intervals were too low to reach any conclusion.

In a further effort to determine whether a change in IRP2 protein could account for the increase in ferritin we observed, we evaluated protein levels by Western blotting using an

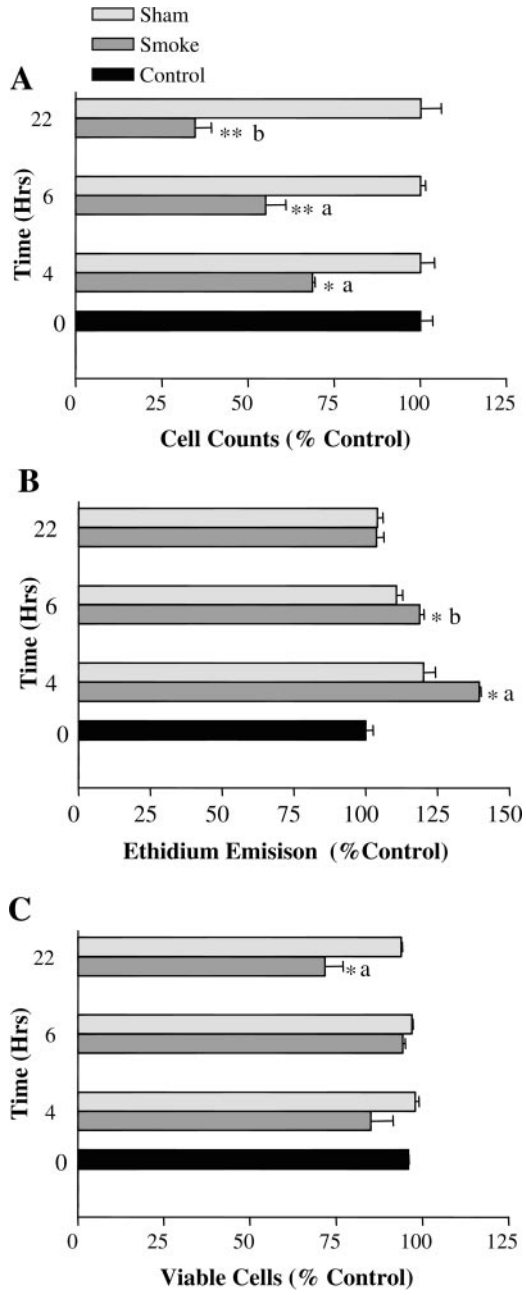

Fig. 3. Effects of smoke on viability of A549 cells. A549 cells were grown to 80% confluence in RPMI medium with serum (5%). Smoke or sham air was delivered at a rate of 6 ml/s for 5 s as described in MATERIALS AND METHODS. Cells were harvested at the appropriate time interval, and viability was determined. *A*: smoke decreases numbers of cells, as determined by hemocytometer. [a]Significantly different from sham-treated cells, $P < 0.002$. [b]Significantly different from sham-treated cells, $P < 0.001$. *Significantly different from control cells, $P < 0.01$. **Significantly different from control cells, $P < 0.001$. *B*: initial numbers of cells are similar in all treatment groups. [a]Significantly different from sham-treated cells, $P < 0.01$. [b]Significantly different from sham-treated cells, $P < 0.05$. *Significantly different from control cells, $P < 0.001$. *C*: surviving cells in all treatment groups are viable. Cells were evaluated as trypan blue positive cells set in ratio to the total number of cells present and taken as a percentage of controls. [a]Significantly different from sham-treated cells, $P < 0.01$. *Significantly different from control cells, $P < 0.05$. Trypan blue exclusion and ethidium assays were conducted as described in MATERIALS AND METHODS. Graphed data represent means ± SE for 3 experiments conducted at the same time.

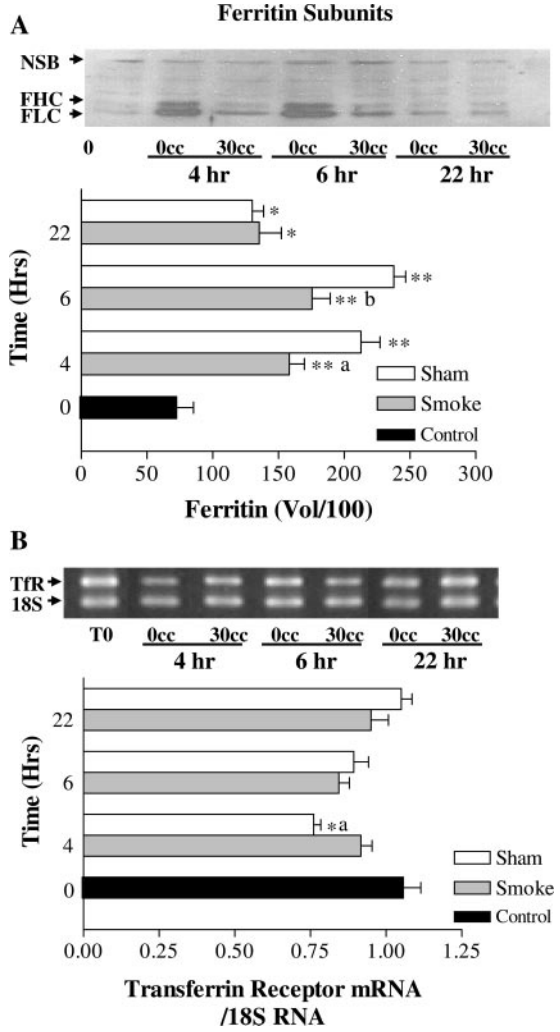

Fig. 4. Ferritin and TfR mRNA levels of A549 cells exposed to smoke or sham air. A549 cells were grown to 80% confluence in RPMI medium with serum (5%). Smoke or sham air was delivered at a rate of 6 ml/s for 5 s as described in MATERIALS AND METHODS. Cells were harvested at the designated time interval. *A*: sham air induces ferritin synthesis; smoke exposure significantly decreases this response. Immunoblots were conducted and analyzed as described in MATERIALS AND METHODS. Ponseau Red staining and nonspecific bands (NSB) revealed by enhanced chemiluminescence (ECL) were used to monitor even loading and transfer. [a]Significantly different from sham-treated cells, $P < 0.03$. [b]Significantly different from sham-treated cells, $P < 0.01$. *Significantly different from control cells, $P < 0.05$. **Significantly different from control cells, $P < 0.01$. *B*: TfR mRNA levels are sustained with smoke treatment. Total RNA isolation and semiquantitative RT-PCR were conducted as described in MATERIALS AND METHODS. Data were analyzed as a ratio of the TfR product to the 18S internal standard. [a]Significantly different from smoke-treated cells, $P < 0.04$. *Significantly different from control cells, $P < 0.01$. Graphed data represent means ± SE for 3 experiments conducted at the same time. A representative panel is shown above the appropriate graph.

IRP2-specific antiserum. We found that IRP2 significantly declined with air or smoke treatment (Fig. 6*A*). The decline in IRP2 corresponded with the changes we observed in ferritin synthesis. We conclude that IRP2 degradation could account for the increased ferritin synthesis we observed for both smoke and sham cells. Although the decrease in IRP2 could also result in a decrease in TfR mRNA, further work on TfR mRNA transcription would be necessary to draw conclusions regarding this parameter.

Smoke is known to contain reactive oxygen species (ROS) as well as iron. We evaluated oxidative byproducts in our culture media by the TBARS assay. As shown in Fig. 6*B*, the levels of oxidative stress introduced by this small amount of smoke did not result in changes in this parameter. We conclude from these data that A549 cells mounted a sufficient response to accommodate the levels of ROS introduced by 30 ml of smoke and that any iron introduced in smoke failed to generate sufficient oxidative stress to produce lipid oxidation byproducts.

We also evaluated expansion of the labile iron pool using calcein fluorescence quench (Fig. 7*A*) and mitochondrial activity by Formazan absorbance (Fig. 7*B*). Calcein fluorescence was not quenched in sham cells at the early time intervals, indicating that uptake of iron from sham air was minimal at these time points. In contrast, calcein levels were significantly lower for smoke-treated cells at all time intervals. However, when calcein fluorescence values were compared with Formazan absorbance or with cell numbers expressed as percentages of appropriate controls, no significant differences were found for either sham (Fig. 7*C*) or smoke-treated (Fig. 7*D*) cells. At 22 h, percentages for calcein fluorescence of sham cells was significantly lower than those obtained by other methods, but not significantly different from controls. A follow-up study of calcein fluorescence in A549 cells demonstrated that calcein fluorescence declines in linear relationship with increasing iron dose (Fig. 7*E*). [For this experiment, no significant differences in numbers of viable cells were found by trypan blue assay (data not shown)]. To substantiate that iron was not responsible for the decline in calcien fluorescence we observed in smoke-treated cells, we attempted to obtain a measurement of iron apart from cell viability. We evaluated calcien fluorescence on cytoplasmic extracts and culture media in the presence or absence of DES (3). Quench levels were very low, and no differences in iron were detected with time or smoke treatment (data not shown). From these data taken together, we conclude that, if iron was introduced by either sham air or smoke, levels were below detection by the calcein assay. The results of the calcein and Formazan assays appeared to accurately reflect the decline in the numbers of viable cells in smoke-treated samples.

DISCUSSION

Adequate iron to meet nutrient needs of most mammalian cells depends on the uptake of ferric transferrin via TfRs. On the other hand, uptake must be limited and the iron stored in ferritin to avoid oxidative stress. This balance is accomplished by an iron-mediated decrease in IRP-IRE interaction that simultaneously upregulates ferritin synthesis and TfR mRNA degradation (10). We have shown that iron delivered at physiological levels dramatically induces ferritin synthesis in A549 cells without reducing TfR mRNA. This coincides with nearly a complete loss of IRP2 binding activity. At higher iron doses, IRP1 binding activity declines and is accompanied by a reduction in TfR mRNA. Thus, for A549 cells, different mechanisms influencing IRP-IRE interaction allow ferritin translation in the presence of TfR mRNA to provide for iron needs and yet prevent potential oxidative stress.

These results support the findings of others of hierarchical regulation of the targets of IRP action (11, 44). Despite low

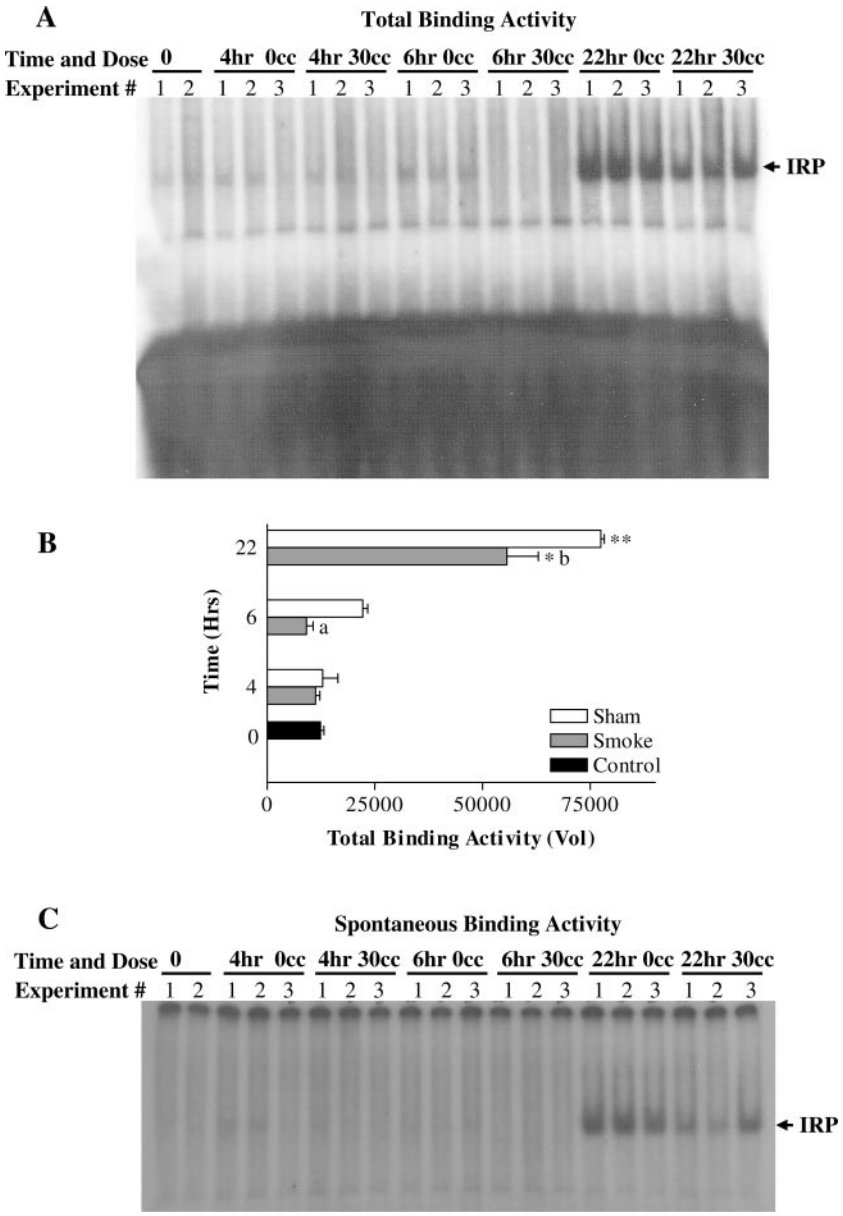

Fig. 5. Total and spontaneous IRP binding activity of A549 cells exposed to smoke or sham air. A549 cells were grown to 80% confluence in RPMI medium with serum (5%). Smoke or sham air was delivered at a rate of 6 ml/s for 5 s as described in MATERIALS AND METHODS. Cells were harvested at the designated time interval. Electrophoretic mobility shift assays were conducted and analyzed as described in MATERIALS AND METHODS. *A* and *C*: A549 cells show minimal binding activity after smoke or sham air treatment at early time intervals. *B*: graphed data of total binding activity of cells treated with smoke or sham air. [a]Significantly different from sham-treated cells, $P < 0.002$. [b]Significantly different from sham-treated cells, $P < 0.05$. *Significantly different from control cells, $P < 0.01$. **Significantly different from control cells, $P < 0.001$. Graphed data represent means ± SE for 3 experiments.

levels of expression, IRP2 appears important in upregulating ferritin synthesis in response to physiological levels of iron without disturbing levels of TfR mRNA in A549 cells. Several studies have shown that IRPs have different affinities for various IRE structures (34, 35, 48). IRP2 binds with greater affinity to the ferritin mRNA IRE than to the IREs of the TfR mRNA; this is attributed to the internal bulge found in the stem of the ferritin IRE (28, 29). The crucial role of IRP2 in controlling ferritin levels in vivo also was indicated in recent studies demonstrating ferritin accumulation in the brains of IRP2 knockout mice (19). The loss of IRP2 binding activity we observed at the low iron dose also implies that IRP2 degradation by the proteosome is sensitive to relatively minor increases in intracellular iron (21, 25).

We were expecting a greater decline in IRP1 binding activity at the lower iron doses. Others have reported that, in some cells, IRP1 is activated by iron in the dose range that we used as a result of oxidative stress (39). We found no evidence of oxidative byproducts in the culture medium. However, the TBARS assay measures only some lipid oxidation byproducts. Further studies using appropriate antioxidants would be necessary to conclude that oxidative stress did not occur. The decline in IRP1 binding activity coincides with downregulation of TfR mRNA and suggests that TfR mRNA levels were regulated by IRP1. This notion would agree with studies that indicate IRP1 and IRP2 bind equally well with the TfR mRNA IREs (13). Regardless of the mechanisms involved, our results show that fine tuning of IRP-IRE binding activity allows A549 cells to respond to a low iron dose by increasing ferritin synthesis while preserving TfR mRNA, a process vital to sustaining intracellular iron stores.

To evaluate the effects of pollution on this system, we exposed A549 cells to cigarette smoke or sham air. We were surprised to discover that sham air stimulated ferritin synthesis at the early time intervals. Our findings indicate that, similar to the dose-response studies, this could be attributed to a decline

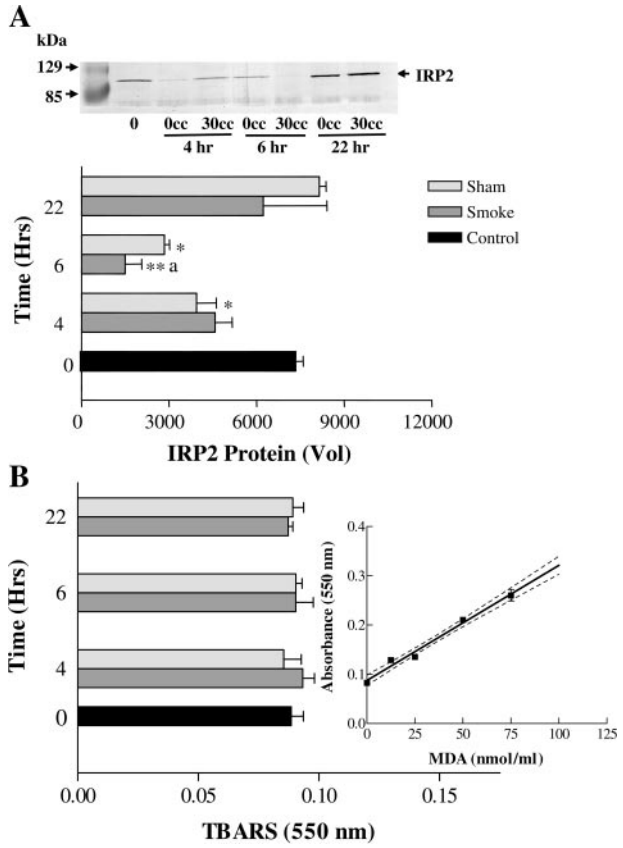

Fig. 6. Response of IRP2 to smoke or sham air. A549 cells were grown to 80% confluence in RPMI medium with serum (5%). Smoke or sham air was delivered at a rate of 6 ml/s for 5 s as described in MATERIALS AND METHODS. Cells were harvested at the designated time interval. *A*: sham air significantly reduces IRP2. Immunoblots were conducted using an anti-IRP2 specific polyclonal antibody (a kind gift from Dr. R. Eisenstein) and analyzed as described in MATERIALS AND METHODS. A nonspecific band at ~85,000 Da was used to monitor even loading and transfer. [a]Significantly different from sham-treated cells, $P < 0.04$. *Significantly different from control cells, $P < 0.01$. **Significantly different from control cells, $P < 0.05$. *B*: smoke treatment does not increase lipid peroxidation. Thiobarbituric acid reactive species assay (TBARS) was conducted as described in MATERIALS AND METHODS. The standard curve is shown in *inset*. Graphed data represent means ± SE for 3 experiments. A representative panel is shown above the graph.

in IRP2 levels. However, the mechanism(s) responsible for the reduction in IRP2 levels by sham air are not clear. The most plausible explanation is that, despite the presence of an inline filter, sufficient iron entered the cells to reduce IRP2. Although calcein fluorescence did not indicate an increase in the labile iron pool, possibly this method was not sufficiently sensitive to measure an increase in intracellular iron from the sham air. Alternatively, IRP2 degradation requires oxygen (27). Recently, Leibold and colleagues demonstrated that oxygen status plays a central role in IRP2 stability (23, 46). These authors found that hypoxia results in an increase in IRP2 binding activity and a decrease in ferritin synthesis. Sham air would not likely change the oxygen levels significantly relative to room air. However, the air delivery technique could have resulted in an increase in oxygen tension at the surface of the cell layer that resulted in IRP2 degradation. The upregulation of IRP-IRE interaction and IRP2 protein at 22 h also could be the result of prolonged exposure to serum-free culture medium. In any case, these data indicate that, for A549 lung cells, subtle changes in environmental conditions alter intracellular iron metabolism. Our findings also suggest that how air is applied to lung cells in culture can impact the results of studies of iron metabolism and that changes in oxygen tension could be an important factor in iron metabolism of this tissue.

We administered a relatively low level of smoke to these cells. Because others have reported that iron is present in airborne smoke particles, we anticipated that the sham air response would be accentuated in smoke-treated cells. Surprisingly, this level of smoke diminished ferritin synthesis and degradation of TfR mRNA. We do not know what mechanisms were responsible for these observations. Cigarette smoke contains superoxide, catachols, and hydroquinones, as well as nitric oxide (18, 31). The effects of superoxide on IRP binding activity are inconclusive because the methods used to impose oxidative stress influence the experimental results. However, work to date suggests that ROS can up- or downregulate IRP1 binding activity, increase IRP2, and increase ferritin synthesis (reviewed in Refs. 1, 9, 10, 24). These changes are not in line with our observations, and we found no evidence of lipid oxidation byproducts in the culture medium. These data suggest that, at this level of smoke, the formation of ROS is minimal and that oxidative stress is not likely responsible for the changes we observed.

Similar to studies of the effects of superoxide, the effects of nitric oxide on intracellular iron metabolism reflect the experimental methods employed. Nitric oxide activates IRP1 binding activity, downregulates IRP2, and can reduce TfR mRNA (reviewed in Refs. 9 and 30). However, recent data indicate that A549 cell ferritin levels are increased in response to nitric oxide (47). Smoke also contains catachols and hydroquinones that can activate protein kinase C (18). Both IRP2 and IRP1 can be phosphorylated by protein kinase C, which activates IRP binding and increases TfR mRNA levels (45). Protein kinase C activation working in concert with nitric oxide could have played a role in diminishing ferritin synthesis and TfR mRNA degradation of smoke-treated cells. However, it seems likely that we also would have observed an increase in total binding activity at the early time intervals if these were the predominate mechanisms responsible for our observations.

Alternatively, the presence of smoke also could have created a mild hypoxic response in A549 cells. Hypoxia has been shown to increase TfR mRNA by upregulation of transcription, to reduce ferritin accumulation, and to stabilize IRP2 in some human cells (23, 46, 50).

We did not evaluate TfR transcription or the cause of A549 cell death after smoke treatment as part of this work. However, future studies evaluating these and other effects of smoke on A549 cells in the presence of appropriate inhibitors and antioxidants will help reveal the mechanisms responsible for the changes in iron metabolism that we observed.

Importantly, regardless of the mechanisms involved, we found that smoke exposure reduced ferritin levels and prevented downregulation of TfR mRNA. Ferritin serves as a cytoprotective agent against oxidative stress (8), and iron delivered by TfRs or by airborne particles can increase oxidative stress (7, 26). Thus repeated exposure of lung tissues to low levels of smoke as are present in environmental pollutants could result in reduced cytoprotection by ferritin at a time when iron uptake is sustained and ROS are present. This could

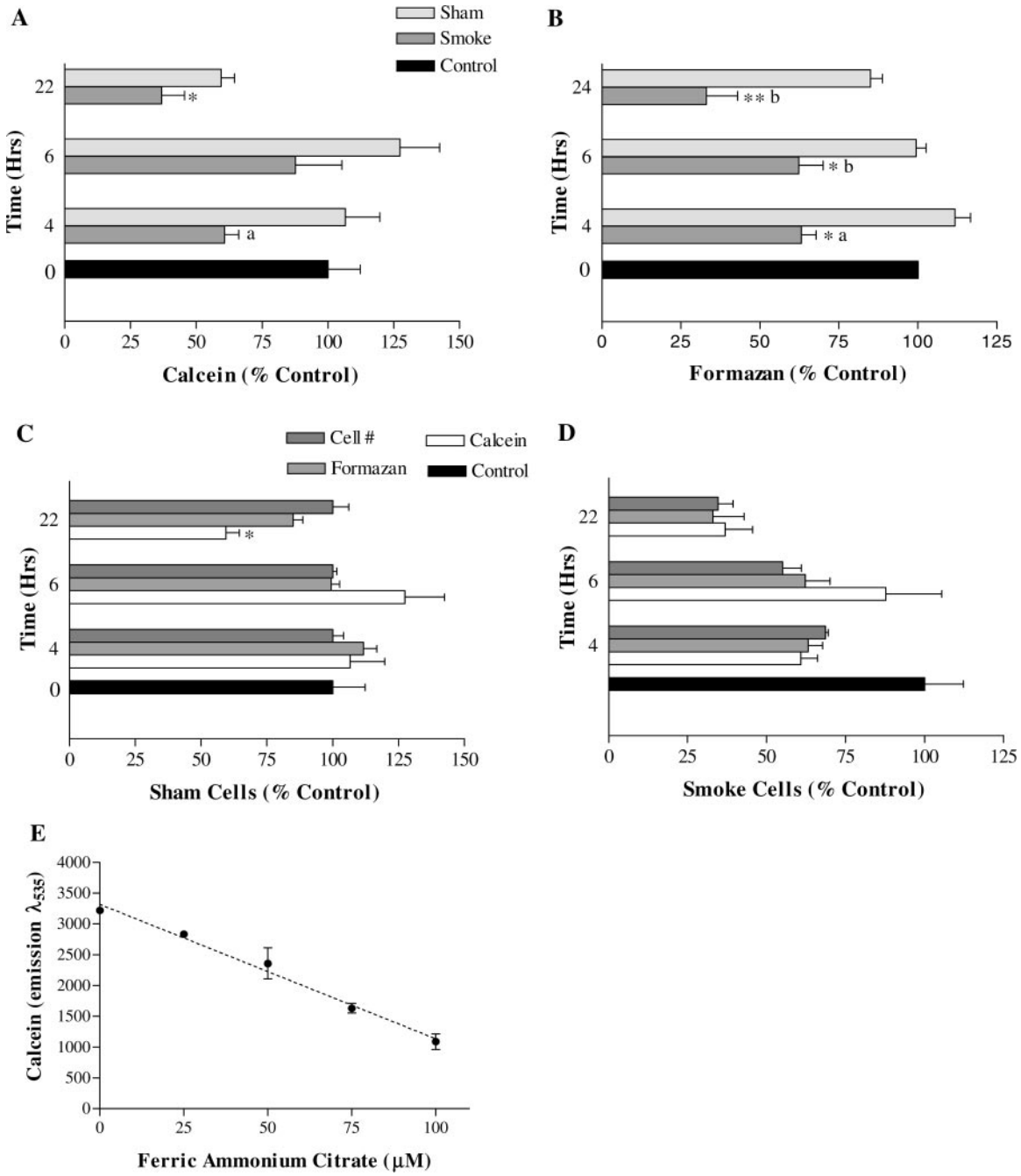

Fig. 7. Effects of smoke on the labile iron pool and mitochondrial activity of A549 cells. A549 cells were grown to 80% confluence in RPMI medium with 5% serum. Smoke or air was delivered at 6 ml/s for 5 s. Cells were harvested as described in MATERIALS AND METHODS. *A*: smoke decreases calcein fluorescence of A549 cells. Calcein assay was conducted as described in MATERIALS AND METHODS and is expressed as a percentage of controls. [a]Significantly different from sham-treated cells, $P < 0.03$. *Significantly different from control, $P < 0.05$. *B*: smoke decreases mitochondrial activity as measured by Formazan absorbance. Formazan assay was conducted as described in MATERIALS AND METHODS and is expressed as a percentage of controls. [a]Significantly different from sham-treated cells, $P < 0.002$. [b]Significantly different from sham-treated cells, $P < 0.01$. *Significantly different from control, $P < 0.05$. **Significantly different from control, $P < 0.001$. *C*: Formazan absorbance and calcein fluorescence reflect numbers of sham cells. Cell number was taken from hemocytometer counts (Fig. 4*A*). All data are expressed as a percentage of appropriate controls (0 h, no air or smoke). *Significantly different from cell counts ($P < 0.006$) and Formazan ($P < 0.015$). *D*: Formazan absorbance and calcein fluorescence reflect numbers of smoke-treated cells. *E*: FAC results in dose-responsive iron uptake as measured by calcein fluorescence quench. Graphed data represent means ± SE for 3 experiments.

enhance the probability of lung damage by iron-mediated oxidative stress.

In summary, we have shown that lung cells adjust iron metabolism in response to environmental stimuli and can serve as a model of the effects of environmental pollutants on intracellular iron metabolism. Our work also indicates that low doses of iron result in ferritin synthesis in A549 cells without degradation of TfR mRNA, a change resulting primarily from

IRP2 reduction. Treatment with sham air also induces ferritin synthesis and decreases IRP2. Studies of the exposure of IRP2 knockout mice to airborne iron particles and to various environmental pollutants could provide more information on the importance of this protein to lung iron metabolism and protection against environmental insult. We also have demonstrated that smoke exposure can decrease ferritin synthesis and increase TfR mRNA levels. These changes could enhance iron-mediated oxidative stress and encourage lung cell damage after smoke exposure.

ACKNOWLEDGMENTS

We thank Theresa Spicer for assistance with the preparation of the manuscript.

GRANTS

Funding for this work was provided by the Arizona Disease Research Commission, the College of Agriculture and Life Sciences, and United States Department of Agriculture Hatch no. 136209-H-22-121 at the Agricultural Experiment Station at the University of Arizona.

REFERENCES

1. **Aisen P, Enns C, and Wessling-Resnik M.** Chemistry and biology of eukaryotinc iron metabolism. *Int J Biochem Cell Biol* 33: 940–959, 2001.
2. **Aisen P, Wessling-Resnick M, and Leibold EA.** Iron metabolism. *Curr Opin Chem Biol* 3: 200–206, 1999.
3. **Ali A, Zhang Q, Dai J, and Huang X.** Calcein as a fluorescent iron chemosensor for the determination of low molecular weight iron in biological fluids. *Biometals* 16: 285–293, 2003.
4. **Ausubel F, Brent R, Kingston RE, Moore DD, Seidman JG, Smith JA, and Stuhl K.** *Current Protocols in Molecular Biology*. New York: Wiley, 1998.
5. **Beinert H, Kennedy MC, and Stout CD.** Aconitase as iron-sulfur protein, enzyme, and iron-regulatory protein. *Chem Rev* 96: 2335–2373, 1996.
6. **Bradford MM.** A rapid and sensitive method for the quantitation of microgram quantities of protein utilizing the principle of protein-dye binding. *Anal Biochem* 72: 248–254, 1976.
7. **Breuer W, Greenberg E, and Cabantchik ZI.** Newly delivered transferrin iron and oxidative cell injury. *FEBS Lett* 403: 213–219, 1997.
8. **Cairo G, Castrusini E, Minotti G, and Bernellizazzera A.** Superoxide and hydrogen peroxide-dependent inhibition of iron regulatory protein activity: a protective stratagem against oxidative injury. *FASEB J* 10: 1326–1335, 1996.
9. **Cairo G and Pietrangelo A.** Iron regulatory proteins in pathobiology. *Biochem J* 352: 241–250, 2000.
10. **Eisenstein RS.** Iron regulatory proteins and the molecular control of mammalian iron metabolism. *Annu Rev Nutr* 20: 627–662, 2000.
11. **Eisenstein RS and Ross KL.** Novel roles for iron regulatory proteins in the adaptive response to iron deficiency. *J Nutr* 133: 1510S–1516S, 2003.
12. **Eisenstein RS, Tuazon PT, Schalinske KL, Anderson SA, and Traugh JA.** Iron-responsive element-binding protein. Phosphorylation by protein kinase C. *J Biol Chem* 268: 27363–27370, 1993.
13. **Erlitzki R, Long JC, and Theil EC.** Multiple, conserved iron-responsive elements in the 3′-untranslated region of transferrin receptor mRNA enhance binding of iron regulatory protein 2. *J Biol Chem* 277: 42579–42587, 2002.
14. **Fang R and Aust AE.** Induction of ferritin synthesis in human lung epithelial cells treated with crocidolite asbestos. *Arch Biochem Biophys* 340: 369–375, 1997.
15. **Foster KA, Oster CG, Mayer MM, Avery ML, and Audus KL.** Characterization of the A549 cell line as a type II pulmonary epithelial cell model for drug metabolism. *Exp Cell Res* 243: 359–366, 1998.
16. **Gangaidzo IT, Moyo VM, Mvundura E, Aggrey G, Murphree NL, Khumalo H, Saungweme T, Kasvosve I, Gomo ZA, Rouault T, Boelaert JR, and Gordeuk VR.** Association of pulmonary tuberculosis with increased dietary iron. *J Infect Dis* 184: 936–939, 2001.
17. **Ghio AJ, Suliman HB, Carter JD, Whorton AR, Piantadosi CA, and Wang X.** Iron uptake and Nramp2/DMT1/DCT1 in human bronchial epithelial cells. *Am J Physiol Lung Cell Mol Physiol* 282: L693–L702, 2002.
18. **Gopalakrishna R, Chen ZH, and Gundimeda U.** Tobacco smoke tumor promoters, catechol and hydroquinone, induce oxidative regulation of protein kinase C and influence invasion and metastasis of lung carcinoma cells. *Proc Natl Acad Sci USA* 91: 12233–12237, 1994.
19. **Grabill C, Silva AC, Smith SS, Koretsky AP, and Rouault TA.** Abstract MRI detection of ferritin iron overload and associated neuronal pathology in iron regulatory protein-2 knockout mice. *Brain Res* 971: 95–106, 2003.
20. **Guo B, Brown FM, Phillips JD, Yu Y, and Leibold EA.** Characterization and expression of iron regulatory protein 2 (IRP2). Presence of multiple IRP2 transcripts regulated by intracellular iron levels. *J Biol Chem* 270: 16529–16535, 1995.
21. **Guo B, Phillips JD, Yu Y, and Leibold EA.** Iron regulates the intracellular degradation of iron regulatory protein 2 by the proteasome. *J Biol Chem* 270: 21645–21651, 1995.
22. **Gurgueira SA, Lawrence J, Coull B, Murthy GG, and Gonzalez-Flecha B.** Rapid increases in the steady-state concentration of reactive oxygen species in the lungs and heart after particulate air pollution inhalation. *Environ Health Perspect* 110: 749–755, 2002.
23. **Hanson ES, Rawlins ML, and Leibold EA.** Oxygen and iron regulation of iron regulatory protein 2. *J Biol Chem* 278: 40337–40342, 2003.
24. **Hentze MW and Kuhn LC.** Molecular control of vertebrate iron metabolism: mRNA-based regulatory circuits operated by iron, nitric oxide, and oxidative stress. *Proc Natl Acad Sci USA* 93: 8175–8182, 1996.
25. **Iwai K, Drake SK, Wehr NB, Weissman AM, LaVaute T, Minato N, Klausner RD, Levine RL, and Rouault TA.** Iron-dependent oxidation, ubiquitination, and degradation of iron regulatory protein 2: implications for degradation of oxidized proteins. *Proc Natl Acad Sci USA* 95: 4924–4928, 1998.
26. **Kamp DW and Weitzman SA.** The molecular basis of asbestos induced lung injury. *Thorax* 54: 638–652, 1999.
27. **Kang D, Jeong J, Drake SK, Wehr NB, Rouault TA, and Levine RL.** Iron regulatory protein 2 as iron sensor. *J Biol Chem* 278: 14857–14864, 2003.
28. **Ke Y, Sierzputowska-Gracz H, Gdaniec Z, and Thiel EC.** Internal loop/bulge and hairpin loop of the iron-responsive element of ferritin mRNA contribute to maximal iron regulatory protein 2 binding and translational regulation in the iso-iron-responsive element/iso-iron regulatory protein family. *Biochemistry* 39: 6235–6242, 2000.
29. **Ke Y and Theil EC.** An mRNA loop/bulge in the ferritin iron-responsive element forms in vivo and was detected by radical probing with Cu-1,10-phenantholine and iron regulatory protein footprinting. *J Biol Chem* 277: 2373–2376, 2002.
30. **Kim S and Ponka P.** Role of nitric oxide in cellular iron metabolism. *Biometals* 16: 125–135, 2003.
31. **LaLonde C, Nayak U, Hennigan J, and Demling R.** Antioxidants prevent the cellular deficit produced in response to burn injury. *J Burn Care Rehabil* 17: 379–383, 1996.
32. **Lay JC, Bennett WD, Ghio AJ, Bromberg PA, Costa DL, Kim CS, Koren HS, and Devlin RB.** Cellular and biochemical response of the human lung after intrapulmonary instillation of ferric oxide particles. *Am J Respir Cell Mol Biol* 20: 631–642, 1999.
33. **Leanderson P and Tagesson C.** Cigarette smoke-induced DNA damage in cultured human lung cells: role of hydroxyl radicals and endonuclease activation. *Chemico-Biological Interactions* 81: 197–208, 1992.
34. **Meehan HA and Connell GJ.** The hairpin loop but not the bulged C of the iron responsive element is essential for high affinity binding to iron regulatory protein-1. *J Biol Chem* 276: 14791–14796, 2001.
35. **Menotti E, Henderson BR, and Kuhn LC.** Translational regulation of mRNAs with distinct IRE sequences by iron regulatory proteins 1 and 2. *J Biol Chem* 273: 1821–1824, 1998.
36. **Muckenthaler M, Gray NK, and Hentze MW.** IRP-1 binding to ferritin mRNA prevents the recruitment of the small ribosomal subunit by the cap-binding complex eIF4F. *Mol Cell* 2: 383–388, 1998.
37. **Nelson ME, Cowley BD Jr, Bailey K, and Wesselius LJ.** Increased release of ferritin and iron by iron-loaded alveolar macrophages in cigarette smokers. *Am J Respir Cell Mol Biol* 12: 275–279, 1995.
38. **Nelson ME, O'Brien-Ladner AR, and Wesselius LJ.** Regional variation in iron and iron-binding proteins within the lungs of smokers. *Am J Respir Crit Care Med* 153: 1353–1358, 1996.

39. **Nunez MT, Nunez-Millacura C, Tapia V, Munoz P, Mazariegos D, Arredondo M, Munoz P, Mura C, and Maccioni RB.** Iron-activated iron uptake: a positive feedback loop meidated by the iron regulatory protein 1. *Biometals* 16: 83–90, 2003.
40. **Ponka P and Lok CN.** The transferrin receptor: role in health and disease. *Int J Biochem Cell Biol* 31: 1111–1137, 1999.
41. **Pope CA 3rd, Burnett RT, Thun MJ, Calle EE, Krewski D, Ito K, and Thurston GD.** Lung cancer, cardiopulmonary mortality, and long-term exposure to fine particulate air pollution. *JAMA* 287: 1132–1141, 2002.
42. **Quinlan GJ, Chen Y, Evans TW, and Gutteridge JM.** Iron signalling regulated directly and through oxygen: implications for sepsis and the acute respiratory distress syndrome. *Clin Sci (Colch)* 100: 169–182, 2001.
43. **Ryan TP, Krzesicki RF, Blakeman DP, Chin JE, Griffin RL, Richards IM, Aust SD, and Petry TW.** Pulmonary ferritin: differential effects of hyperoxic lung injury on subunit mRNA levels. *Free Radic Biol Med* 22: 901–908, 1997.
44. **Schalinske KL, Chen OS, and Eisenstein RS.** Iron differentially stimulates translation of mitochondrial aconitase and ferritin mRNAs in mammalian cells. Implications for iron regulatory proteins as regulators of mitochondrial citrate utilization. *J Biol Chem* 273: 3740–3746, 1998.
45. **Schalinske KL and Eisenstein RS.** Phosphorylation and activation of both iron regulatory proteins 1 and 2 in HL-60 cells. *J Biol Chem* 271: 7168–7176, 1996.
46. **Schneider BD and Leibold EA.** Effects of iron regulatory protein regulation on iron homeostasis during hypoxia. *Blood* 102: 3404–3411, 2003.
47. **Smith JJ, O'Brien-Ladner AR, Kaiser CR, and Wesselius LJ.** Effects of hypoxia and nitric oxide on ferritin content of alveolar cells. *J Lab Clin Med*: 309–317, 2003.
48. **Theil EC and Eisenstein RS.** Combinatorial mRNA regulation: iron regulatory proteins and iso-iron-responsive elements (Iso-IREs). *J Biol Chem* 275: 40659–40662, 2000.
49. **Thompson AB, Bohling T, Heires A, Linder J, and Rennard SI.** Lower respiratory tract iron burden is increased in association with cigarette smoking. *J Lab Clin Med* 117: 493–499, 1991.
50. **Toth I, Yuan L, Rogers JT, Boyce H, and Bridges KR.** Hypoxia alters iron-regulatory protein-1 binding capacity and modulates cellular iron homeostasis in human hepatoma and erythroleukemia cells. *J Biol Chem* 274: 4467–4473, 1999.
51. **Winzerling JJ, Jouni ZE, and McNamara DJ.** Human peritoneal monocytic cells: lipoprotein uptake and foam cell formation. *Life Sci* 62: 501–513, 1998.